PHYSICAL REVIEW B VOLUME 26, NUMBER 7 1 OCTOBER 1982

Nuclear tracks in iron garnet films

P. Hansen and H. Heitmann
Philips GmbH Forschungslaboratorium Hamburg, D-2000 Hamburg 54, West Germany

P. H. Smit
Philips Research Laboratories, Eindhoven, The Netherlands
(Received 22 February 1982)

Epitaxial iron garnet films of composition $Y_3Fe_5O_{12}$, $Gd_3Fe_5O_{12}$, and $(Gd,Bi)_3(Fe,Ga)_5O_{12}$, irradiated with xenon or uranium ions of energies 1.4 and 6 MeV per nucleon exhibit nuclear tracks of lengths between 10 and 30 μm. These tracks were studied by saturation magnetization measurements and conversion electron Mössbauer spectroscopy elucidating a strong crystallographic disorder and a paramagnetic behavior in the track volume. The track diameter depends on mass and energy of the ions used for irradiation and was found to range between 15 and 20 nm for the energies investigated.

I. INTRODUCTION

The irradiation of nonconducting solids with heavy ions of high energy leads to the formation of nuclear tracks.[1] These have been discussed in nonmagnetic materials and in particular with respect to various applications.[1-3] The physical picture that has emerged is the following. The heavy ion that enters the solid is stripped, to a large extent, of its electrons and thus is highly positively charged. It ionizes the lattice ions along its trajectory. The induced high charge density leads to a Coulomb explosion where the positively charged lattice ions are ejected perpendicular to the trajectory of the heavy ion. This leads to the formation of a nuclear track of cylindrical shape, in which the ionic density is expected to be somewhat reduced at the center and increased towards the outer regions.[1] Thus strong local distortions and strain throughout the irradiated region are the result.[4] However, little information is available about the atomic arrangement in the track volume. Magnetic materials offer additional possibilities to study the track structure. In particular magnetic oxides such as iron garnets can give detailed information since the superexchange interaction is very sensitive with respect to changes of the crystallographic ordering and therefore most of the magnetic properties are also expected to be strongly affected by these tracks. This indeed was found from saturation-magnetization measurements of bismuth-substituted gadolinium iron garnet films which could only be explained assuming a complete destruction of the magnetic ordering in the track volume.[5] Thus significant changes of the atomic arrangement must have taken place, which is in accordance with the irradiation-induced change of the lattice mismatch measured between epitaxial garnet films and their single-crystal substrates.[4] Other magnetic properties such as the Faraday rotation,[6,7] the ferromagnetic resonance linewidth,[7] the uniaxial anisotropy,[8] and the domain-wall coercivity[7,9,10] are also influenced very strongly by the presence of nuclear tracks. From these properties, however, conclusions about the nature of the tracks can be drawn only indirectly. Therefore, in this work we have focused our attention to the measurement of the saturation magnetization which reflects average changes in the superexchange interactions and to conversion-electron Mössbauer measurements which reveal changes in the local magnetization. The magnetization measurements were extended to different garnet compositions to confirm the preliminary results reported in Ref. 5 and to ions of differing mass and energy.

II. EXPERIMENTS

A. Garnet films

The garnet films of composition $Y_3Fe_5O_{12}$, $Gd_3Fe_5O_{12}$, and $Gd_{1.7}Bi_{1.3}Fe_{4.3}Ga_{0.7}O_{12}$ have been grown on (111)-oriented substituted gadolinium gallium garnets. The $Y_3Fe_5O_{12}$ films used for the Mössbauer measurements are 25% enriched in ^{57}Fe ions.[11] The film thickness ranged between 2.5 and 6.3 μm. Discs of 0.5- and 1.5-cm diameter were cut from the original samples for the magnetization and Mössbauer measurements, respectively. These discs had been irradiated with xenon ions (^{132}Xe), having

an energy per nucleon of 1.4 and 6 MeV/u (corresponding to 185 and 792 MeV per ion, respectively) and uranium ions (^{238}U) of 1.4 MeV/u (333 MeV per ion).[12] The dosage level d ranged between 10^{10} and 10^{12} per cm^2. For the energy of 6 MeV/u it was difficult to exceed values of d larger than 5×10^{11} cm^{-2}, since for higher dosage levels the samples tend to crack into small pieces due to the high internal stresses. The length of the induced nuclear tracks of approximately cylindrical shape was found to range between 10 and 30 μm for these energies.[13,14] In Fig. 1 the situation after bombardment is sketched, where the thickness of the tracks is enlarged by a factor of roughly 10. A high degree of overlap of the tracks occurs for dosage levels larger than 3×10^{11} cm^{-2}. The average track diameter is constant in the epitaxial film provided the track length is significantly larger than the film thickness. This holds for the considered energies per nucleon in the range 1 to 10 MeV/u, since for garnets in this range the energy loss dE/dx reaches its maximum value, resulting in an approximately constant value for dE/dx vs x, and thus for the track radius within the first microns.

From Fig. 1 it can be expected that these nuclear tracks in particular affect the domain-wall motion, which will be reflected in the equilibrium domain configuration for sufficiently high dosage levels. This is indeed what we observed and it may serve as a simple example to demonstrate the influence of the tracks on the magnetic properties. In Fig. 2 the domains of an uniaxial bismuth-substituted gadolinium iron garnet film are displayed where the circular area has been irradiated with uranium ions of 1.4 MeV/u. The sample has been heated up and then cooled back to room temperature. Since the nuclear tracks act as pinning centers for the domain walls the domain configuration in the irradiated area is fixed and cannot redistribute itself, in contrast to the nonirradiated surrounding area. Since the track diameter is small ($\sim$20 nm) (Refs. 1 and 5) compared to the domain-wall thickness, dosage levels larger than 3×10^{10} cm^{-2} are necessary to obtain a sufficient wall pinning.

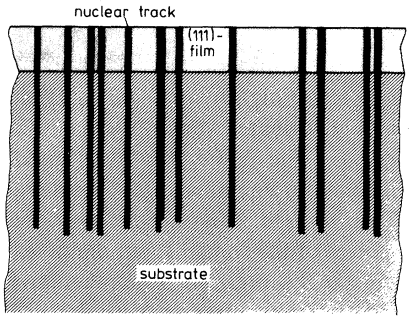

FIG. 1. Schematic representation of nuclear tracks in iron garnet films. Thickness of the tracks is exaggerated by a factor of 10 as compared to the film thickness.

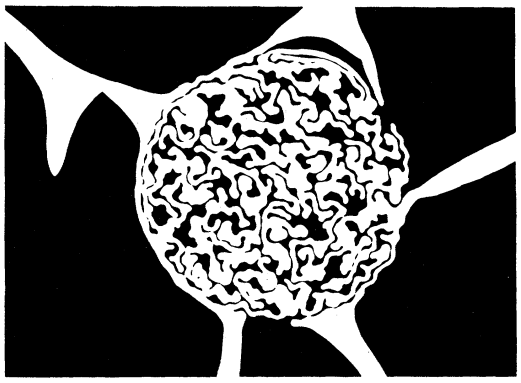

FIG. 2. Domain pattern of a bismuth-substituted gadolinium iron garnet film being irradiated (circular area) with uranium ions of energy 1.4 MeV per nucleon (333 MeV per ion). Film was heated and then cooled to room temperature. Since the nuclear tracks act as pinning centers for the domain walls the domain pattern in the circular area cannot redistribute during cooling and therefore represents the equilibrium distribution corresponding to the elevated temperature.

B. Saturation magnetization

The magnetization measurements were carried out with a vibrating sample magnetometer in the temperature range 4.2 K $\leq T \leq T_C$ and in fields up to 20 kG. Some results are shown in Fig. 3. The

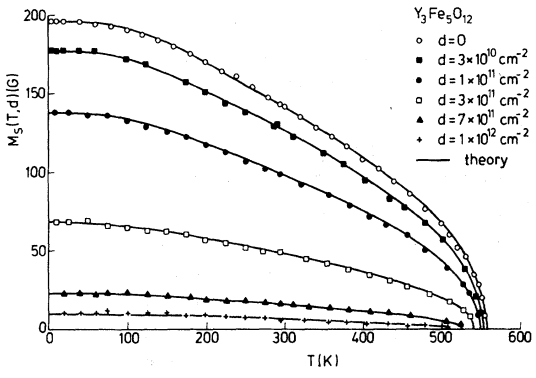

FIG. 3. Temperature dependence of the saturation magnetization for yttrium iron garnet irradiated with uranium ions of energy 1.4 MeV per nucleon for different dosage levels. Solid lines were calculated from the molecular-field theory.

data were obtained from extrapolation to zero field. All samples possess the same volume and therefore changes of the saturation magnetization $M_s(T,d)$ caused by the formation of nuclear tracks can be expressed by[5]

$$M_s(T,d)=M_s(T,0)\exp[-\sigma(R_m)d]\,, \qquad (1)$$

where $M_s(T,0)$ is the magnetization at temperature T before irradiation. $\sigma(R_m)L=\pi R_m^2 L$ represents the volume of the track, which for films of constant thickness L is determined by the track radius R_m of the paramagnetic cylinder only. The exponential dependence accounts for the overlap of the tracks for high dosage levels d.

The temperature dependence of $M_s(T,d)$ is controlled by the Brillouin function.[5,15] The measured temperature dependence of $M_s(T,d)$ for the yttrium iron garnet, irradiated with ^{238}U of 1.4 MeV/u is shown in Fig. 3. The approach of $M_s(T,d)$ to $M_s(0,d)$ indicates that no magnetic ordering occurs within the tracks, since $M_s(0,d)$ is smaller than $M_s(0,0)$. Antiferromagnetism or spin-glass-type behavior, however, cannot be excluded.

In the high-temperature range ($T\gtrsim 400$ K) the curves indicate a linear reduction of the Curie temperature with increasing dose. However, the experimental accuracy, in particular for high dosage levels, is not too good and therefore the dependence of T_C on d is less accurate. The theoretical curves in Fig. 3 were calculated assuming the molecular-field coefficients to decrease with increasing d.

From the magnetization data at the same reduced temperatures the average track diameter $2R_m$ can be determined. Rewriting Eq. (1) in the form

$$\pi R_m^2 d=\ln\left[\frac{M_s(T,0)}{M_s(T,d)}\right], \qquad (2)$$

R_m is obtained from the slope of a logarithmic plot of the ratio of the magnetizations at $T=20$ K. For all compositions investigated these relations are shown in Fig. 4 for different energies and masses of the heavy ions used for irradiation. The track diameters $2R_m$ determined from these plots are given in Table I. We estimate the standard deviations in the R_m values to be ± 0.4 nm which primarily are

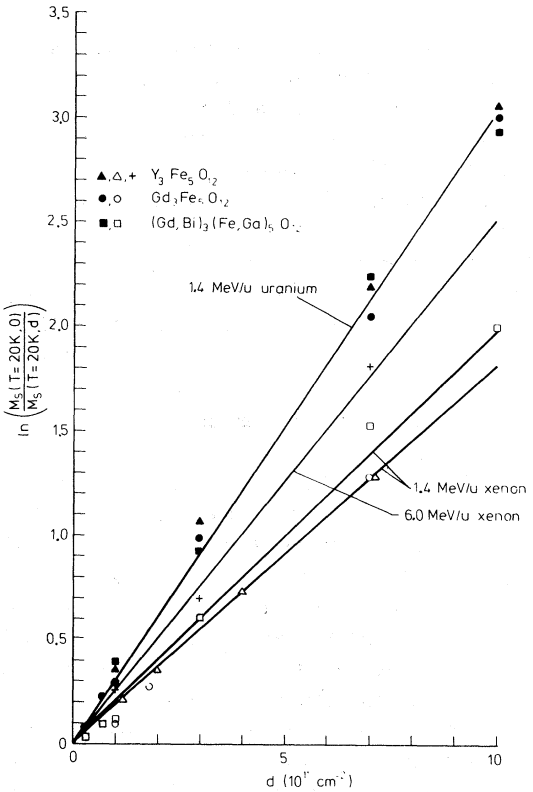

FIG. 4. Logarithmic plot of the magnetization vs dosage level according to Eq. (2) for the different garnets investigated. From the slope the magnetic radius R_m of the tracks can be deduced.

TABLE I. Nuclear track diameters in iron garnets induced by irradiation with xenon and uranium ions. R_m is determined from the magnetization measurements, and R_p from the Mössbauer spectra. Estimated standard deviations in $2R_m$ and $2R_p$ are ± 0.8 nm.

Ion	Energy per nucleon (MeV)	Garnet composition	$2R_m$ (nm)	$2R_p$ (nm)
^{132}Xe	1.4	$Y_3Fe_5O_{12}$	15.2	13.4
		$Gd_3Fe_5O_{12}$	15.2	—
		$Gd_{2.3}Bi_{0.7}Fe_{4.3}Ga_{0.7}O_{12}$[a]	15.2	—
		$Gd_2BiFe_{4.3}Ga_{0.7}O_{12}$	15.8	—
^{132}Xe	6	$Y_3Fe_5O_{12}$	17.8	—
^{238}U	1.4	$Y_3Fe_5O_{12}$	19.7	17.4
		$Gd_3Fe_5O_{12}$	19.7	—
		$Gd_{1.7}Bi_{1.3}Fe_{4.3}Ga_{0.7}O_{12}$	19.7	—

[a]Taken from Ref. 5.

caused by the inaccuracy of d.

It turns out that there is almost no dependence of R_m on the garnet composition. However, R_m depends on the ion energy and mass in accordance with the energy loss per unit length of the heavy ions in solids. Xenon ions of 1.4 MeV/u produce track radii that are about 17% smaller than the radii caused by 6-MeV/u xenon ions.

The influence of the mass is even greater. Almost doubling the nuclear mass at the same energy per nucleon results in an increase of R_m by 30%.

C. Mössbauer measurements

The ^{57}Fe conversion-electron Mössbauer (CEM) spectra were recorded on a conventional constant-acceleration spectrometer with a ^{57}Co in Pd source using a gas-flow proportional counter to collect the electrons. In this way the electrons are detected without energy discrimination, and they are mainly K-conversion and Auger electrons, the great majority of which emerge from a depth of less than 100 nm.[16] Also detected are the L- and M-conversion electrons, which come from deeper-lying layers and Compton and photoelectrons which are created by resonantly emitted x rays and γ rays in the bulk of the film.[17,18] As a consequence, a ^{57}Fe CEM spectrum will be composed mainly of contributions from the first 100 nm and partly from contributions from deeper-lying layers (estimated to be about 25%).[18]

The hyperfine field at the iron nuclei, which is proportional to the sublattice magnetization, can be deduced from the separation of the lines in the ^{57}Fe Mössbauer spectrum. From the intensity ratios of the peaks the direction of the hyperfine field and thus of the magnetization can be deduced. The intensity ratios of the outer, middle and inner pairs of peaks in a sextet is $3(1+\cos^2\theta):4\sin^2\theta:(1+\cos^2\theta)$ where θ is the angle between the incident γ rays and the hyperfine field. In this work the γ rays are perpendicular to the film and the magnetization of the nonirradiated $Y_3Fe_5O_{12}$ film is almost parallel to the film plane ($\theta=10°-90°$). For iron garnets a superposition of the subspectra originating from the tetrahedral and octahedral sublattices is present as shown in Fig. 5(a). Owing to the arbitrary direction of the magnetization with respect to the symmetry directions of the tetrahedral and octahedral sites, several different quadrupole and hyperfine splittings are present. This results in slightly different subspectra from crystallographically inequivalent sites. In Figs. 5(b)–5(e) the spectra of $Y_3Fe_5O_{12}$ films after irradiation with ^{238}U and ^{132}Xe are presented.

It can be seen that ion-bombardment results in a paramagnetic fraction, exhibiting itself as a doublet in the middle of the spectrum. The intensity of the doublet increases with dose, as expected. In order to determine the absolute fraction of the film which is rendered paramagnetic, the observed spectra were least-squares-fitted with two sextets and one doublet. From the areas of the two sextets and the doublet a paramagnetic radius R_p can be determined assuming a circular cross section for the track. R_p is then given by

$$\pi d R_p^2 = \ln\left[\frac{I_{\text{sextets}}+I_{\text{doublet}}}{I_{\text{sextets}}}\right], \tag{3}$$

where I indicates the spectrum area. We find for ^{132}Xe, $R_p=6.7$ nm, and for ^{238}U, $R_p=8.7$ nm. The standard deviation in R_p is estimated to be at most ± 0.4 nm. Since these R_p values are smaller than the R_m values calculated from the saturation-magnetization data, there appears to be a region which does not contribute to M_s and at the same time does not show up in the paramagnetic doublet. It was checked that the Mössbauer fraction of the Fe ions in the paramagnetic region did not significantly differ from that of the Fe ions in the undisturbed lattice. The relative intensities of the second and fifth lines, which decrease with increasing dose for ^{238}U bombardment, show that in parts of the film the magnetization is rotated towards the film normal, i.e., parallel to the track axes. Especially in the case of 5.1×10^{11} ^{238}U ions per cm^2 [Fig. 5(e)] is this clearly visible, and it indicates that local perpendicular anisotropies are introduced by the ion bombardment. In the case of Xe irradiation this does not happen. Here it should be noticed that the total intensity of the Mössbauer spectrum is independent of the magnetic state of the iron ions with respect to d.

The linewidths of the irradiated $Y_3Fe_5O_{12}$ are somewhat broadened after the ions have entered the lattice. This is to be expected since a considerable amount of strain is introduced by the bombardment.[4] The situation is quite different from that after lower-energy ion implantation (100–300 keV per ion), where the lattice is more or less homogeneously affected.[11,19] The paramagnetic doublet has an isomer shift (IS) of 0.29 mm s^{-1} with respect to α-Fe, which is practically the average value of IS in unperturbed $Y_3Fe_5O_{12}$ and a quadrupole splitting (QS) of 1.2 mm s^{-1}. These values are, within 0.1 mm s^{-1}, the same as found after high-dose ion implantation[19] and as measured for amorphous roller-

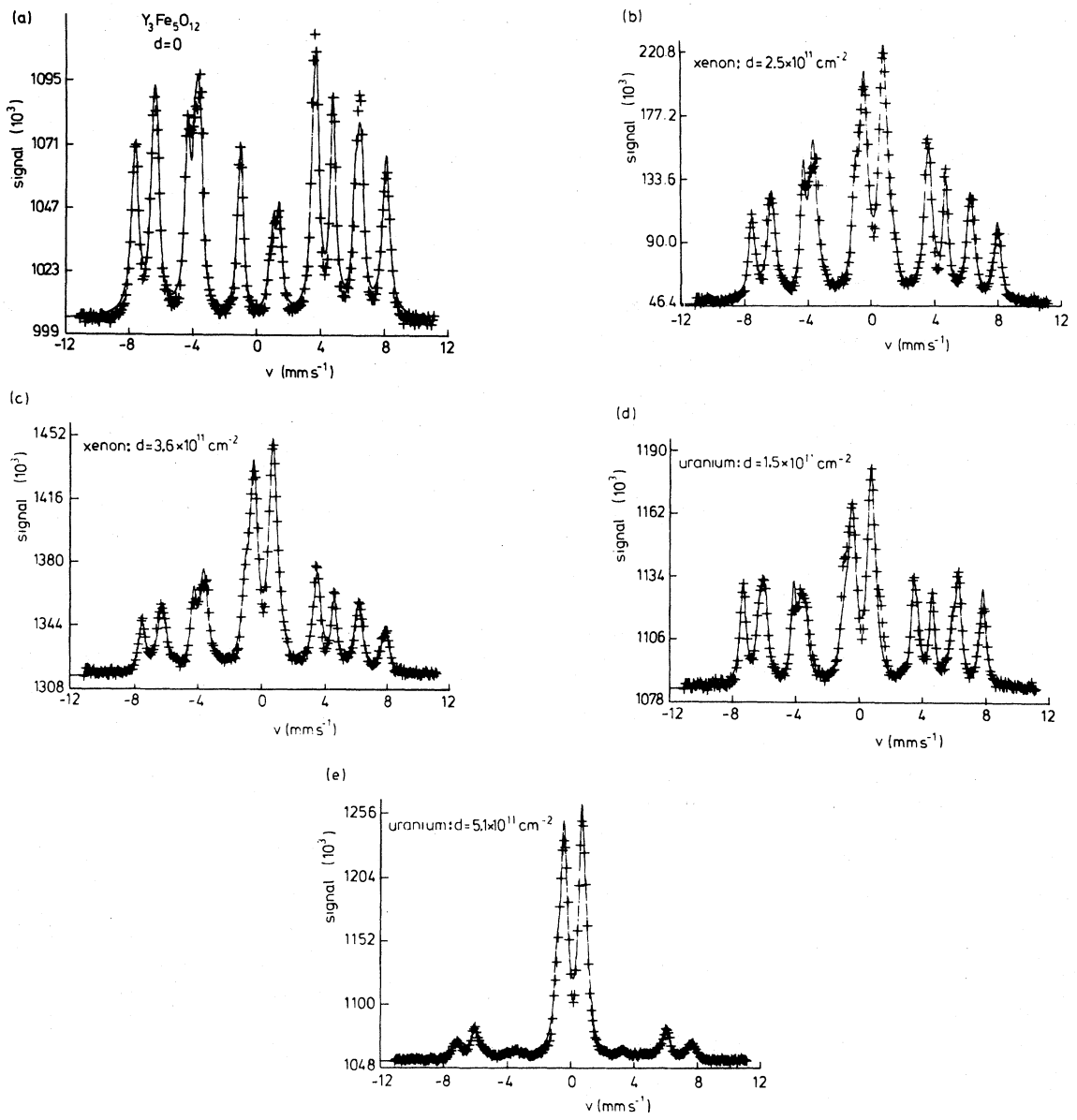

FIG. 5. ^{57}Fe conversion-electron Mössbauer spectra for $Y_3Fe_5O_{12}$ at $T=295$ K. Incident γ rays were perpendicular to the (111)-film plane. (a) nonirradiated film; (b) and (c) films irradiated with xenon ions of energy 1.4 MeV per nucleon (185 MeV per ion); (d) and (e) films irradiated with uranium ions of energy 1.4 MeV per nucleon (333 MeV per ion).

quenched $Y_3Fe_5O_{12}$.[20] Ferric ions apparently are not very sensitive to the precise structure of their immediate surrounding as far as these quantities are concerned.

III. DISCUSSION

The experimental observations may be summarized as follows:

(i) The high-energy heavy-ion irradiation reduces the average magnetic moment by the factor $\exp[-\sigma(R_m)d]$, and the magnitude of this factor depends on the energy and mass of the incident ions.

(ii) In the track the superexchange interaction is destroyed and the magnetic ions behave as in a paramagnetic system.

(iii) There appears to be a transition range between the paramagnetic track and the undistorted

lattice, where the superexchange interaction is restored, and which does not contribute to the net magnetization.

(iv) A small reduction of the Curie temperature and the exchange interaction is present.

The dependence of the track diameter on the energy and mass of the incident ions is in accordance with the energy loss dE/dx of heavy ions in solids[21] which is proportional to the square of the projectile charge. This dependence is well approximated by the Bethe-Bloch relation[1,21] in the energy range discussed here. Thus dE/dx is proportional to the distorted volume or to R_m^2. For the ^{132}Xe and ^{238}U ions in garnets dE/dx has a maximum in the range between 2.5 and 4 MeV/u and it decreases for higher energies.[21] Therefore, an increase of the primary energy from 1.4 to 6 MeV/u tends to increase the track length but should not lead to a drastic change of the diameter. For ^{132}Xe and film thicknesses ranging between 2.5 and 6.3 μm the average values, $\overline{dE/dx}$, increased by 30% in the considered energy range which is in good agreement with the observed change of R_m by 17%. Ions of higher mass, however, are characterized by higher values of dE/dx. At an energy of 1.4 MeV/u, $\overline{dE/dx}$ for ^{238}U is about 60% higher than that for ^{132}Xe which again is reflected in the observed R_m data being 30% larger for the ^{238}U ion. From the energy-loss function it is expected that light ions do not produce tracks. Irradiation of garnets with helium ions of energy 1 to 3.5 MeV/u (Ref. 22) indeed failed to produce measurable changes of the magnetization.

We are now in a position to refine the model proposed earlier.[5] From the CEM spectra we know that the core of the track, which is paramagnetic, has a radius of $R_p = 8.7 \pm 0.4$ nm in the case of 1.4-MeV/u uranium ions. From the M_s values we found that the track radius, defining the border between the surrounding unaffected garnet and the material in the track area which does not contribute to the measured magnetizations, is $R_m = 9.9 \pm 0.4$ nm. Although the difference in R_m and R_p is small the magnetic data strongly support the presence of a transition range of thickness $R_m - R_p$. The material inside this transition range gives rise to a normal $Y_3Fe_5O_{12}$ Mössbauer spectrum, but has a net magnetization of zero. Moreover, in the case of ^{238}U irradiation the direction of the hyperfine fields is no longer in the plane of the film but has a component parallel to the film normal. The M_s values were measured in a magnetic field parallel to the plane. If there are large anisotropies induced in this transition region the highest magnetic field used in this study of 20 kOe will not be able to align these magnetic moments and they will not contribute to the magnetization. The same effect would result from a quasiantiferromagnetic ordering in this transition region. We therefore consider the tracks to consist of two magnetic regions, as indicated in Fig. 6. In Fig. 6(a) the strong damage of the lattice induced by the process of the Coulomb explosion is sketched. This leads to a radial dependence of the relative defect density $d(R)$ (Ref. 23) indicated by the dashed-dotted line in Fig. 6(b). $d(R)$ is determined by the presence of different types of defects.[24] Within a radius of $R_p \leq 8.7$ nm, $d(R)$ is high and thus the material behaves paramagnetically. At $d(R_p)$ the defect density is sufficiently low and the superexchange interaction is restored. In the transition region between R_p and R_m the material is either ferrimagnetic with strong local anisotropies, where in the case of ^{238}U a preferential axis along the film normal is present, or a quasiantiferromagnetic state is present owing to the distortion of the lattice. For the ^{132}Xe bombardment the situation is similar. The radius of the paramagnetic region is about 10% smaller than that of the nonmag-

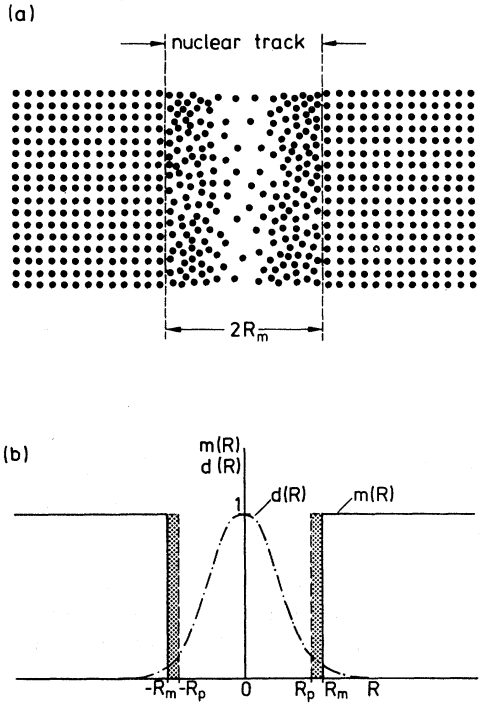

FIG. 6. (a) Schematic representation of a nuclear track created by Coulomb explosion and (b) the radial dependence of the relative defect density $d(R)$ and the relative magnetization $m(R) = M_s(R)/M_s(\infty)$ in the track (see text).

netic radius, just as for ^{238}U. No preferential direction of the anisotropy is observed, however.

The presence of this thin transition range between distorted and undistorted lattice is in good agreement with results from healing experiments.[25] It shows that the magnetic nuclear track radius is well defined and thus is expected to be a good measure to characterize the track dimensions. It should be noted that R_m is larger than the radius deduced from electron transmission experiments ($2R = 11$ nm for $Y_3Fe_5O_{12}$ irradiated with ^{132}Xe of 1.4-MeV/u ions).[26]

IV. CONCLUDING REMARKS

The irradiation of iron garnet films with heavy ions of high energy leads to the creation of nuclear tracks. Magnetization and Mössbauer measurements reveal that the superexchange interaction causing the ferrimagnetic ordering is destroyed in the track volume. The track diameter is almost independent of the garnet composition. It is primarily determined by the mass of the heavy ions and only slightly by their energy. A transition region of thickness $R_m - R_p$ exists between the paramagnetic core of the nuclear track and the surrounding undistorted lattice. $R_m - R_p$ is about 10% of the magnetic track radius R_m and thus the transition from the paramagnetic to the ferrimagnetic state is rather abrupt.

Further it should be noted that the scattering mechanisms of magnons and phonons could be investigated at well-defined defects like the cylindrically shaped nuclear tracks. For this purpose the significantly increased etching rate along the track axes can be used to produce cylinders of diameters ranging between about 0.01 and 10 μm. The etching behavior of the tracks combined with appropriate diffusion processes, in addition, offers new possibilities in the fields of technical applications such as microstructuring, three-dimensional structures or the control of magnetic and electric properties.

ACKNOWLEDGMENTS

The authors would like to thank W. Tolksdorf and J. M. Robertson for the growth and preparation of the garnet films, R. Spohr from the Gesellschaft für Schwerionenforschung Darmstadt for the irradiation with xenon and uranium, L. Blatt and P. E. Wigen from Ohio State University for the helium irradiation, and J. Schuldt for technical assistance. The authors are grateful to R. P. van Stapele for the critical reading of the manuscript. The work described was sponsored by the German Federal Ministry for Research and Technology (BMFT) under Grant No. 2007/3.

[1]R. L. Fleischer, P. B. Brice, and R. M. Walker, *Nuclear Tracks in Solids: Principles and Applications* (University of California Press, Berkeley, 1975).

[2]C. Hepburn and A. H. Windle, J. Mater. Sci. 15, 279 (1980).

[3]R. Spohr, J. Electrochem. Soc. 128, 188 (1981); Nucl. Instrum. Methods 173, 229 (1980).

[4]B. Strocka, G. Bartels, and R. Spohr, J. Appl. Phys. 21, 141 (1980).

[5]P. Hansen and H. Heitmann, Phys. Rev. Lett. 43, 1444 (1979).

[6]H. Heitmann, P. Hansen, R. Spohr, and K. Witter, J. Magn. Magn. Mater. 15-18, 1543 (1980).

[7]H. Heitmann, P. Hansen, and R. Spohr, IEEE Trans. Magn. MAG-17, 2979 (1981).

[8]H. Dötsch, C. Vittoria, and H. Heitmann, IEEE Trans. Magn. MAG-17, 2982 (1981).

[9]H. Heitmann, C. Fritzsche, P. Hansen, J.-P. Krumme, R. Spohr, and K. Witter, J. Magn. Magn. Mater. 7, 40 (1978).

[10]H. Heitmann, P. Hansen, R. Spohr, and K. Witter, J. Magn. Magn. Mater. 10, 97 (1979).

[11]P. H. Smit, H. A. Algra, and J. M. Robertson, J. Appl. Phys. 22, 299 (1980).

[12]The irradiation has been performed at the Gesellschaft für Schwerionenforschung (GSI), Darmstadt, Germany.

[13]J.-P. Krumme, B. Strocka, Ch. Schmelzer, R. Spohr, and K. Witter, J. Appl. Phys. 48, 5191 (1977).

[14]K. Thiel, H. Külzer, and W. Herr, Nucl. Track Detection 2, 127 (1978).

[15]P. Röschmann and P. Hansen, J. Appl. Phys. 52, 6257 (1981).

[16]D. Liljequist, T. Ekdahl, and U. Bäverstam, Nucl. Instrum. Methods 155, 529 (1978).

[17]M. J. Tricker, L. A. Ash, and T. E. Cranshaw, Nucl. Instrum. Methods 143, 307 (1977).

[18]F. A. Deeney and P. J. McCarthy, Nucl. Instrum. Methods 166, 491 (1979).

[19]P. H. Smit, H. A. Algra, and J. M. Robertson, J. Appl. Phys. 52, 2364 (1981).

[20]E. M. Gyorgy, K. Nassau, M. Eibschütz, J. V. Waszczak, C. A. Wang, and J. C. Shelton, J. Appl. Phys. 50, 2883 (1979).

[21]L. C. Northcliffe and R. F. Schilling, Nucl. Data Tables Sect. A 7, 233 (1970).

[22]The helium irradiation was carried out by Professor L. Blatt, Ohio State University, Coulombus, Ohio.

[23]R. L. Fleischer, *Progress in Materials Science* (Pergamon, New York, 1981), p. 97 (Chalmers Anniversary Volume).
[24]E. Dartyge, J. P. Durand, Y. Langevin, and M. Maurette, Phys. Rev. B 23, 5213 (1981).
[25]H. Heitmann and P. Hansen, J. Appl. Phys. (in press).
[26]M. P. A. Viegers and B. Strocka, Appl. Phys. Lett. (in press).